

ITF1697, a Stable Lys-Pro-Containing Peptide, Inhibits Weibel-Palade Body Exocytosis Induced by Ischemia/Reperfusion and Pressure Elevation

Silvia Bertuglia,¹ Hideo Ichimura,² Gianluca Fossati,³ Kaushik Parthasarathi,² Flavio Leoni,³ Daniela Modena,³ Piero Cremonesi,³ Jahar Bhattacharya,² and Paolo Mascagni³

¹CNR Institute of Clinical Physiology, Medical School, University of Pisa, Pisa, Italy; ²Lung Biology Laboratory, St. Luke's-Roosevelt Hospital Center, Columbia University, New York, NY, USA; ³Italfarmaco Research Centre, Cinisello Balsamo, Milan, Italy

A number of Lys-Pro-containing short peptides have been described as possessing a variety of biological activities in vitro. Because of limited metabolic stability, however, their efficacy in vivo is uncertain. To exploit the pharmacological potential of Lys-Pro-containing short peptides, we synthesized a series of chemically modified forms of these peptides. One of them, ITF1697 (Gly-(N α -Et)Lys-Pro-Arg) was stable in vivo and particularly efficacious in experimental models of disseminated endotoxemia and of cardiovascular disorders. Using intravital fluorescence microscopy, we studied the peptide cellular and molecular basis of protection in the Syrian hamster cheek pouch microcirculation subjected to ischemia/reperfusion (I/R) and in pressure elevation-induced proinflammatory responses in isolated Sprague-Dawley rat lungs. Continuous intravenous infusion of ITF1697 at 0.1 to 100 μ g/kg/min nearly completely protected the cheek pouch microcirculation from I/R injury as measured by decreased vascular permeability and increased capillary perfusion. Adhesion of leukocytes and platelets to blood vessels was strongly inhibited by the peptide. ITF1697 exerted its activity at the early stages of endothelial activation and inhibited P-selectin and von Willebrand factor secretion. Further mechanistic studies in the rat lung preparation revealed that the peptide inhibited the intracellular Ca²⁺-dependent fusion of Weibel-Palade bodies with the plasma membrane. The ability of ITF1697 to inhibit the early functions of activated endothelial cells, such as the exocytosis of Weibel-Palade bodies, represents a novel and promising pharmacological tool in model of pathologies of a variety of microvascular disorders.

Online address: <http://www.molmed.org>

doi: 10.2119/2007-00079.Bertuglia

INTRODUCTION

Several biologically active small peptides contain the Lys-Pro motif at the core of their sequence. They include tuftsin (Thr-Lys-Pro-Arg), a γ -globulin derived tetrapeptide that stimulates phagocytosis (1); another tetrapeptide of sequence Gly-Lys-Pro-Val, which corresponds to the C-terminal region of α MSH and is endowed with anti-inflammatory properties (2); and the interleukin-1 β -derived tripeptide Lys-Pro-Thr, which partially antagonizes the hyperalgesic effect of the parent mole-

cule (3). Furthermore, synthetic Lys-Pro-containing peptides (for example, Thr-Lys-Pro-Leu, Gly-Lys-Pro-Arg, and Thr-Lys-Pro-Gln) derived from the sequence of C-reactive protein (CRP), the prototypic acute-phase protein in humans, were shown to possess biological activity (4,5). The pharmacological relevance of these peptides is often uncertain due to their rapid proteolytic degradation in vivo.

To further explore the pharmacological potentials of Lys-Pro-containing peptides, we prepared a number of tri-

and tetrapeptide analogs, which were chemically modified so as to increase their resistance to proteolysis. Among the molecules made, we examined Gly-(N α -Et)Lys-Pro-Arg (ITF1697). ITF1697 has a half-life in vivo of 20 to 120 min, depending on the host species, and greatly reduces mortality and tissue damage in lipopolysaccharide (LPS)-induced systemic endotoxemia and coronary ischemia and ischemia/reperfusion (I/R) (6). The peptide mechanism of action is not known, although evidence has accumulated indicating that cell tissue infiltration is largely inhibited in the presence of ITF1697.

To further understand this protective mechanism, we examined the functional, cellular, and molecular changes induced by I/R in the hamster cheek pouch (7,8) and by pressure elevation in

Address correspondence and reprint requests to Paolo Mascagni, Italfarmaco Research Centre, Via dei Lavoratori 54, Cinisello Balsamo 20092, Milan Italy. Phone: + 390264433001; fax: + 390266011579; e-mail: p.mascagni@italfarmaco.com

Submitted July 16, 2007; accepted for publication October 9, 2007.

Contributed by: Charles A Dinarello.

isolated blood-perfused rat lung preparations (9,10) in response to treatments with ITF1697. Significant increase in microvascular perfusion and decreased vascular permeability after post-ischemic reperfusion were seen in treated animals. Also, I/R-induced endothelium leukocyte and platelet adhesion was prevented in the presence of ITF1697. The mechanism of protection was shown to involve the intracellular Ca^{2+} -dependent fusion of Weibel-Palade bodies with the plasma membrane and the release of P-selectin and von Willebrand factor (vWF) contained in this organelle. Exocytosis of Weibel-Palade bodies is a hallmark of the early stages of endothelial inflammation, and its inhibition may constitute a new and promising target for the treatment of a variety of microvascular disorders.

MATERIALS AND METHODS

The investigation conforms with the Guide for the Care and Use of Laboratory Animals published by the US National Institutes of Health (NIH publ. no. 85-23, revised 1996).

Reagents

ITF1697 and its main metabolite ITF1841 were synthesized as described (6) and were of GMP grade (purity >99%).

I/R of the Hamster Cheek Pouch

Experimental groups. Male Syrian hamsters (80–100 g, Charles River, Italy) were anesthetized (Nembutal, 5 mg/100 g intraperitoneally) and given tracheotomies. The right carotid artery and left femoral vein were cannulated to measure blood pressure and to administer additional anesthesia and drug, respectively. Mean blood pressure was measured by a transducer (Viggo-Spectramed P10E2), and heart rate was monitored using a Gould Windograf recorder.

Animals were subjected to I/R as follows: atraumatic microvascular clips were placed on the proximal part of the cheek pouch to achieve complete ischemia (30 min). The clamp was removed and the microcirculation observed dur-

ing the reperfusion period (30 min). The control group (I/R, $n = 20$) was subjected to I/R and treated with saline. The treatment groups were subjected to I/R and received ITF1697 intravenously infused at 0.1 ($n = 20$), 1 ($n = 20$), and 100 ($n = 30$) $\mu\text{g}/\text{kg}/\text{min}$ or ITF1841 at 10 ($n = 4$) or 100 ($n = 4$) $\mu\text{g}/\text{kg}/\text{min}$. Infusion started 10 min before ischemia and was continued throughout reperfusion. vWF plasma levels were measured on stored plasma from 10 animals from each of the ITF1697 groups and from sham-operated animals ($n = 3$), which were used to determine the background level of vWF induced by anesthesia and surgical treatment. In the time-dependent experiments, 5 animals were used in each experimental group. Additional groups were used to determine P-selectin expression at baseline and I/R in the absence (PS, $n = 7$) and presence of ITF1697 (100 $\mu\text{g}/\text{kg}/\text{min}$, $n = 7$) or ITF1841 (100 $\mu\text{g}/\text{kg}/\text{min}$, $n = 15$) infused intravenously 10 min before ischemia and in the presence of anti-P selectin antibody (CD62-P, $n = 7$).

Fluorescence microscopy. The left cheek pouch of anesthetized hamsters was fixed to the microscope plexiglas platform. Ringer's solution (pH 7.35, 36°C, equilibrated with 5% CO_2 in 95% N_2) was suffused continuously. Observations were made with a Leitz Orthoplan microscope as described (7,11). Fluorescein-bound dextran (molecular weight 150,000) was injected intravenously (500 mg/kg) in 5 min, visualized with a COHU 5253 SIT camera, and subjected to digital image analysis (Project Engineering, Italy).

Capillary perfusion. The perfused capillary length (PCL), defined as the length of capillaries that have transit of at least 1 red blood cell (RBC) in a 30-s period, measured using our laboratory imaging software system, was analyzed in 4 to 6 different microscopic fields (7,8,11). Microvascular diameters (D) and RBC velocity were analyzed online using the photodiode/cross-correlator system (Velocity Tracker 102B; Vista Electronics). The measured centerline velocity was

corrected according to vessel size to obtain the mean RBC velocity (V) (12). Blood flow (Q) was calculated from measured parameters as $Q = VD^2\pi/4$. Wall shear stress (WSS) was calculated from: $WSS = 8\eta V_m/D$, where η , the plasma viscosity, was 1.2 cP at 37°C.

Microvascular permeability. To quantify the permeability of the venular wall, fluorescence intensity in the perivascular space was measured as normalized to baseline gray levels (NGL): $NGL = (I - I_r)/I_r$, where I is the average baseline gray level and I_r is the same parameter after reperfusion (8). Gray levels ranging from 0 to 255 were measured using our laboratory imaging software. The size of the window used to measure average fluorescence intensity was 50 by 50 μm .

Leukocyte and platelet adhesion. Animals received an intravenous injection of acridine red (1 mg/100 g) to visualize leukocytes. Adherent leukocytes were expressed as the number of cells/100 μm length of venule (diameter $16 \pm 8 \mu\text{m}$, length >250 μm). Adherent platelets were expressed as number/ mm^2 of vessel surface (diameter $16 \pm 8 \mu\text{m}$). In each animal, at least 5 arterioles and 5 venules were observed.

P-selectin determination. Two intravenous injections each of anti-human CD62-P polyclonal antibody (Pharmin; 100 μg) and fluorescein-conjugated anti-rabbit IgG (Pharmin; 140 μg) were administered at the beginning and after 15 min of reperfusion. P-selectin secretion was measured as reported (11). Briefly, the fluorescence signal was amplified by a photomultiplier (Hamamatsu R928P-Vista Electronics) and a voltage divider-power supply socket assembly (Hamamatsu C6270). The signal output from the photomultiplier was calibrated as the number of detected photons per unit area of emission. To establish background signal generated by the FITC-labeled secondary antibody, a group of animals was injected with this antibody alone (control). The signal-to-noise ratio was estimated to be on the order of 100:1. Fluorescence in these experiments was detected in the range of 0.1 to 0.5

volts with a window size of 5 by 5 μm . P-selectin expression was expressed as volt/100 μm microvessel.

von Willebrand Factor determination. Plasma vWF levels were determined by ELISA and expressed as percentage according to the manufacturer's instructions (Gradipore, Australia). Plasma citrated samples were taken through the femoral artery catheter during baseline, after declamping, and after 30 min of reperfusion and stored at -80°C until use.

Isolated Blood-Perfused Rat Lung Model

Rat lung preparation. Lungs removed from anesthetized Sprague-Dawley rats (3.5% halothane inhalation and 35 mg/kg intraperitoneal sodium pentobarbital) were continuously pump-perfused with autologous rat blood (14 mL/min) at 37°C . Lungs were constantly inflated with positive airway pressure of 5 cmH_2O . At baseline, pulmonary artery (P_{PA}) and left atrial (P_{LA}) pressures were adjusted to 10 and 5 cmH_2O , respectively. Infusions into the capillary bed were instituted through a microcatheter (PE-10; Baxter) that was advanced through the left atrium and wedged into the venous system. To establish the high-pressure condition, P_{LA} was increased to 15 cmH_2O for 10 min by adjusting the height of the venous outflow. ITF1697 infusion (30 $\mu\text{g}/\text{mL}$) through the microcatheter was initiated 20 min before the baseline period or before pressure challenge, then maintained throughout. The infusion rate (1 mL/h) gives 0.5 $\mu\text{g}/\text{min}$ of ITF1697 infusion.

Fluorescence microscopy. Vehicle for dyes was HEPES buffer (150 mmol/L Na^+ , 5 mmol/L K^+ , 1.0 mmol/L Ca^{2+} , 1 mmol/L Mg^{2+} , and 20 mmol/L HEPES at pH 7.4) containing 4% dextran (70 kDa) and 1% FBS. FM1-43 was used in vehicle without 1% FBS. All monoclonal antibodies and ITF1697 were diluted in Ringer's solution containing 4% dextran (70 kDa; Pharmacia) and 1% FBS (Gemini BioProducts).

Fluorophores were excited by mercury lamp illumination directed through

appropriate filters. Fluorescence emission was collected through objective lens (LUMPlan FI X40; Olympus) and dichroic and emission filters by imaging intensifier (Midnight Sun, Imaging Research, Canada) and video camera (CCD-72; Dage-MTI), then subjected to digital image analysis (MCID-M5, Imaging Research, Canada). The cytosolic Ca^{2+} concentration ($[\text{Ca}^{2+}]_i$) in endothelial cells was quantified using our fura-2 ratiometric imaging technique. Fura-2AM (Molecular Probes; 10 μM) was infused for 20 min via a microcatheter. Fluorescence images were obtained every 10 s during baseline ($P_{\text{LA}} = 5 \text{ cmH}_2\text{O}$) and high-pressure conditions ($P_{\text{LA}} = 15 \text{ cmH}_2\text{O}$), each held for 10 min. Imaging was conducted during a control sequence (no drug infusion) and a test sequence in which infusion of ITF1697 was initiated 20 min before the baseline period, then maintained throughout.

Exocytosis. To quantify exocytosis, FM1-43 (Molecular Probes; 4 μM in dextran-Ringer's solution) was infused for 15 to 20 min via microcatheter into venular capillaries, and fluorescence images were obtained (excitation at 490 nm). After control images were taken, ITF1697 was infused for 35 to 40 min. After 20 min of infusion, FM1-43 was added to ITF1697 and fluorescent images were taken again. The capillaries were maintained under blood-free conditions.

P-selectin determination. P-selectin expression was determined using in situ immunofluorescence methods in non-fixed capillaries. Anti-rat P-selectin monoclonal antibody (RP-2, kindly provided by C. Issekutz, Dalhousie University, Halifax, Nova Scotia, Canada; 3.5 $\mu\text{g}/\text{mL}$) was infused via microcatheter for 4 min, followed by infusion of Alexa Fluor 488 labeled secondary antibody (Molecular Probes; 10 $\mu\text{g}/\text{mL}$) for 4 min. After a 1-min flush with Ringer's solution, residual fluorescence indicative of P-selectin expression was monitored every 10 s until complete loss of the fluorescence signal. This protocol

was repeated at P_{LA} of 5 and 15 cmH_2O in the same vessel with or without ITF1697 treatment.

Leukocyte accumulation. To detect leukocyte accumulation in lung venular capillaries, the leukocyte localizing fluorophore, Rhodamine 6G (Molecular Probes; 1 μM) was added to the perfusion solution. After 20 min, single venular capillaries were imaged at P_{LA} of 5 or 15 cmH_2O in the presence or absence of ITF1697 treatment. After ITF1697 treatment, the microcatheter was removed to reinstate blood flow.

Statistical Analysis

All reported values are means \pm SD. GraphPad Software (San Diego, CA) was used to analyze statistical differences. Statistical differences between groups at the same time points were determined by Kruskal-Wallis followed by Dunn test. Friedman 2-way ANOVA by rank test was used to determine differences between groups at different times, followed by Dunnett test. Differences were considered significant at $P < 0.05$.

RESULTS

I/R in the Hamster Cheek Pouch

Baseline values of mean arterial pressure and heart rate were $87 \pm 7 \text{ mmHg}$ and $310 \pm 20 \text{ beats}/\text{min}$, respectively, and did not change after I/R in sham-operated animals. The doses of ITF1697 [0.1, 1, and 100 $\mu\text{g}/\text{kg}/\text{min}$ (ITF01, ITF1 and ITF100, respectively)] were selected on the basis of preliminary experiments and previous I/R and thrombosis models in rats and hamsters (6) where the peptide was inactive at doses $< 0.1 \mu\text{g}/\text{kg}/\text{min}$.

Effects of I/R and ITF1697 Treatment on Microvascular Parameters

The effects of I/R on the microcirculation parameters are shown in Figures 1 and 2 and summarized in Table 1. Arteriolar diameter decreased significantly during both I/R (Table 1) as did blood flow, which changed from $1.38 \pm 0.7 \text{ nl}\cdot\text{s}^{-1}$ at baseline to $0.69 \pm 0.4 \text{ nl}\cdot\text{s}^{-1}$ after reperfu-

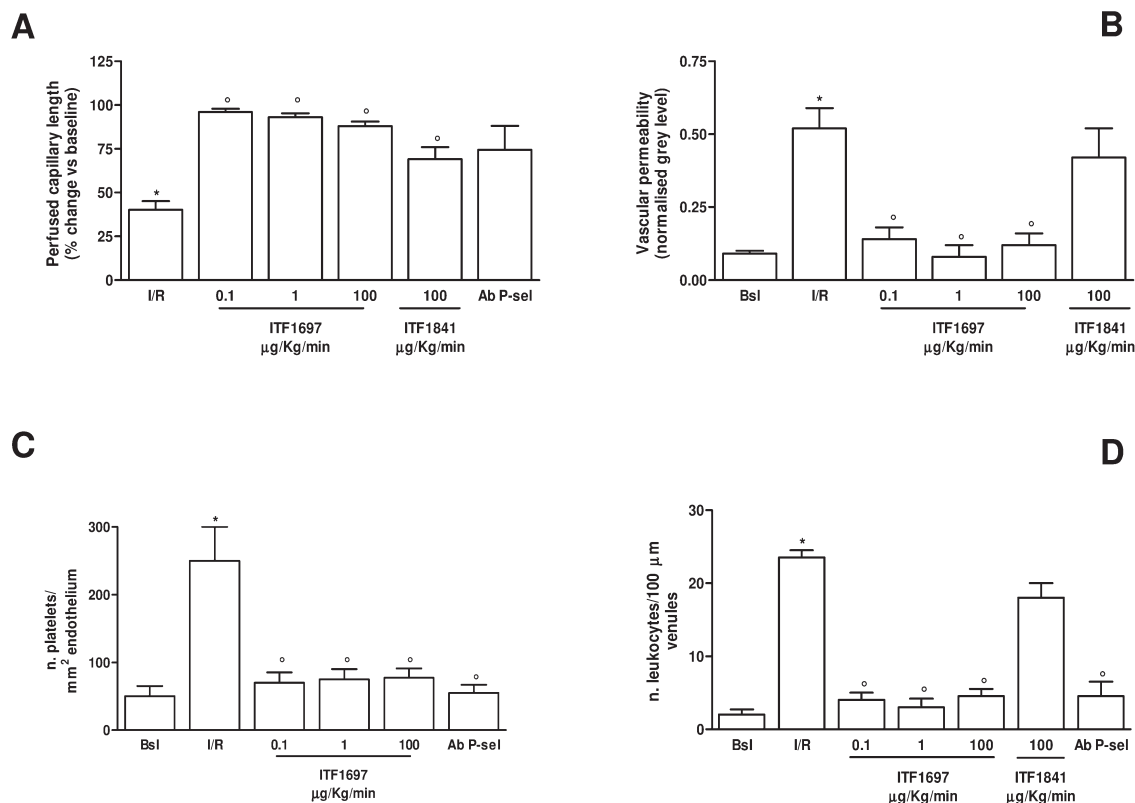


Figure 1. ITF1697 preserves capillary integrity and inhibits I/R-induced platelet and leukocyte adhesion. (A) Changes in perfused capillary length at the end of reperfusion in the I/R, ITF1697, and ITF1841 groups. Values are means \pm SD, $n = 10$ animals per group. * $P < 0.01$ vs. baseline, $^{\circ}P < 0.05$ vs. the I/R group. (B) Vascular permeability at baseline (Bsl) and at the end of reperfusion in the I/R, ITF1697, and ITF1841 groups. Values are means \pm SD, $n = 10$ animals per group. * $P < 0.05$ vs. baseline; $^{\circ}P < 0.05$ vs. the I/R group. (C,D) Platelet (C) and leukocyte (D) adhesion at baseline (Bsl) and at the end of reperfusion in the groups receiving saline (I/R) or ITF1697 at the indicated doses. Adherent platelets per mm² vessel surface and leukocytes per 100 μ m venules are quantified. Values are means \pm SD, $n = 35$ observations for each entry. * $P < 0.05$ vs. baseline; $^{\circ}P < 0.05$ vs. the I/R group.

sion (Table 1). RBC velocity decreased significantly in arterioles (Table 1) but not in venules with diameters of 16 ± 8 ($n = 15$) and $50 \pm 8 \mu\text{m}$ ($n = 15$). Capillary perfusion was largely hampered by I/R, as measured by PCL (Table 1 and Figure 1A), and this was accompanied by a marked increase in permeability of postcapillary and collecting venules (Figures 1B, 2A, and 2B).

ITF1697 treatment either prevented I/R-induced arteriolar vasoconstriction (ITF01; Table 1) or led to a small but significant increase of vasodilation in the ITF1 and ITF100 groups compared with baseline values (Table 1). Although not statistically significant, this trend might reflect a vasodilating effect of the pep-

tide at high doses and/or the existence of a small amount of ischemia in the model at baseline. Whereas peptide-induced vasodilation seems to be less likely due to its lack of effect on mean arterial blood pressure (see above), a small degree of ischemia at baseline might not be totally excluded given the traumatic procedures that the model requires. Thus at high doses ITF1697 might counteract the trauma-induced activation of the circulation.

Arteriolar RBC velocity and blood flow were restored to baseline levels after treatment with all doses of ITF1697 (Table 1). WSS, which decreased after I/R, returned to baseline after ITF1697 treatment (Table 1). PCL was also re-

stored to nearly 100% in the ITF1697-treated groups (Figure 1A), and I/R-induced microvascular permeability was fully inhibited by all dosages of the peptide (Figure 1B). The protective effect of ITF1697 was specifically exerted on the ischemic microvasculature (Figure 2D) and not due to systemic vascular effects as measured by heart rate and mean arterial blood pressure, which did not vary during treatment with ITF1697 compared with baseline conditions.

ITF1841 (Gly-(N α -Et)Lys-Pro), the main metabolite of ITF1697, with modest to null activity in models of myocardial ischemia and I/R, had a modest effect on I/R-induced PCL (Figure 1A) and permeability changes (Figure 1B).

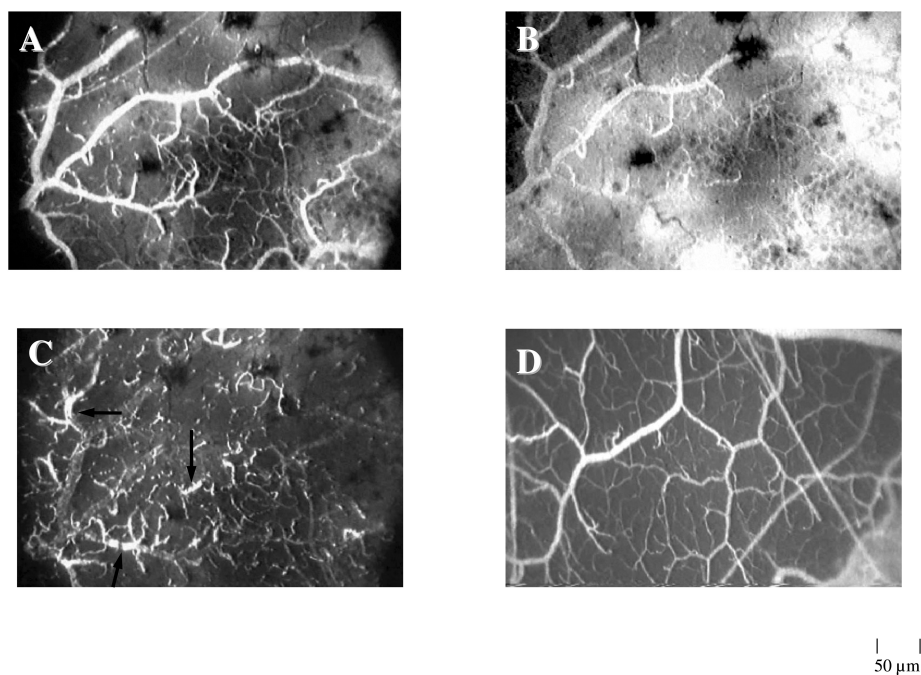


Figure 2. Microvascular modifications during ischemia and reperfusion in the hamster cheek pouch. A microvascular field of a control animal subjected to I/R is visualized using fluorescent dextran after 15 min (A) and 30 min (B) of reperfusion. Diffuse fluorescence outside the vessels indicates extensive plasma extravasation. In the same field, platelets within venules were visualized after 30 min of reperfusion (C), and black arrows indicate extensive blood clotting and platelet adhesion. ITF1697 treatment led to an almost complete inhibition of plasma extravasation after 30 min of reperfusion (D), with no sign of blood clotting or platelet adhesion.

Effects of I/R and ITF1697 Treatment on Platelet and Leukocyte Adhesion

The number of platelets adhering to arterioles and venules and the number of leukocytes adhering to postcapillary venules increased significantly after I/R treatment compared with controls (Table 1 and Figure 1C and D). Increased platelet aggregation at 15 and 30 min of reperfusion led to blood clotting and caused obstruction of venules (Figure 2C). Treatment with ITF1697 restored platelet adhesion to arterioles and venules (Figure 1C) and leukocyte adhesion to postcapillary venules (Figure 1D) to baseline values. In contrast, ITF1841 had a small and non-significant effect on leukocyte adhesion when infused at 10 (not shown) and 100 (Figure 1D) $\mu\text{g}/\text{kg}/\text{min}$.

ITF1697 treatment led to an almost complete inhibition of I/R-induced ex-

travasation, with no sign of blood clotting and platelet adhesion (Figure 2D).

P-Selectin and vWF Secretion

P-selectin and vWF are vasoactive substances secreted by activated endothelial cells that contribute to cellular adhesion to microvessel lumens. Plasma levels of vWF increased by 34% and 91% immediately after declamping and after 30 min of reperfusion, respectively (Figure 3). Similarly, I/R induced significant accumulation of P-selectin on venules and arterioles, mainly at branching points (not shown), reaching peak levels within 15 to 30 min of reperfusion (Figure 4A).

ITF1697 treatment (100 $\mu\text{g}/\text{kg}/\text{min}$) inhibited I/R-induced vWF release and P-selectin expression in arterioles and venules (Figures 3 and 4A) and prevented endothelial leukocyte and platelet adhesion as described above (not

shown). Similar effects were seen when a P-selectin-specific antibody was used, although there was a reduced effect on capillary perfusion compared with ITF1697 treatment (Figure 1A, C, and D). In contrast, ITF1841 (100 $\mu\text{g}/\text{kg}/\text{min}$) led to only partial abrogation of I/R-induced P-selectin expression measured at the end of the reperfusion period (Figure 4B).

Time Course Experiments

Next, we performed time course experiments to determine when ITF1697 was affecting its improvements in microvascular function after injury. When infusion of ITF1697 (1 $\mu\text{g}/\text{kg}/\text{min}$) was started either 15 min after the beginning of ischemia or immediately after reperfusion, the capillary network remained perfused (Table 1). This result is similar to that seen when treatment is begun before ischemia, although improvements in vascular permeability with these delayed treatments were not as good as with treatment before ischemia (Table 1). Administration of the peptide 3 min after reperfusion was less protective than other timings, as shown by a marked increase in permeability, perfusion of the capillary network, and leukocyte adhesion (Table 1).

Isolated Blood-Perfused Rat Lung Model

Secretion of P-selectin by endothelial cells is governed by the regulated exocytosis of Weibel-Palade (WP) bodies. The kinetics of in vivo P-selectin appearance in the vessel lumen is consistent with the secretion of the preformed adhesion molecules stored in WP bodies without a contribution of de novo protein synthesis (13). In addition to P-selectin, WP bodies contain multimeric vWF, which is released with P-selectin upon endothelial activation. The inhibition of P-selectin and vWF secretion observed with ITF1697 treatment indicates that the peptide may block the activation processes leading to WP body secretion and, therefore, the fusion of WP bodies to the plasma membrane. The fusion can be ob-

Table 1. Vascular parameters measured at the end of reperfusion after treatment with ITF1697 either before I/R or after the beginning of ischemia and/or reperfusion

	Pretreatment ^a					Beginning of treatment ^b		
	Control		0.1 µg/kg/min	1 µg/kg/min	100 µg/kg/min	-15 min	0 min	3 min
	Baseline	Reperfusion						
Diameter of Arterioles, µm	30.8 ± 7	14.8 ± 6.5 ^c	30.18 ± 1.2 ^d	32.4 ± 8 ^d	35.7 ± 6 ^d			
RBC velocity, mm/s	2.1 ± 0.25	1.0 ± 0.45 ^c	2.0 ± 0.70 ^d	2.2 ± 0.70 ^d	2.0 ± 0.45 ^d			
Permeability (gray level)	0.09 ± 0.01	0.52 ± 0.07 ^c	0.14 ± 0.04 ^d	0.08 ± 0.04 ^d	0.12 ± 0.04 ^d	0.32 ± 0.05 ^{c,f}	0.35 ± 0.03 ^{c,f}	0.45 ± 0.03 ^{c,f}
Platelets/mm ² endothelium surface	50 ± 15	250 ± 50 ^c	70 ± 15 ^d	75 ± 15 ^d	77 ± 14 ^d			
Leukocytes/100 µm venules	2.0 ± 0.7	23.5 ± 3 ^c	4 ± 1.0 ^d	3 ± 1.2 ^d	4.5 ± 1 ^d	4.5 ± 1.5 ^{e,g}	5.5 ± 1.5 ^{e,g}	7.8 ± 1.9 ^{e,g}
PCL, mm	9.8 ± 0.5	3.8 ± 0.4 ^e	9.41 ± 0.2 ^d	9.07 ± 0.2 ^d		8.2 ± 0.2 ^h	8.31 ± 0.23 ^h	8.03 ± 0.28 ^h
WSS, Pa	0.69 ± 0.33	0.37 ± 0.5 ^c		0.68 ± 0.5	0.64 ± 0.4			
Blood flow (nL·s)	1.38 ± 0.7	0.69 ± 0.4 ^c	1.6 ± 0.4 ^d	1.7 ± 0.5 ^d	1.5 ± 0.5 ^d			

^a10 min before I/R. ^bInfusion (1 µg/kg/min) started 15 min after beginning of ischemia (-15 min), immediately after beginning of reperfusion (0 min), or 3 min after reperfusion (3 min). ^c*P* < 0.05 vs. baseline; ^d*P* < 0.05 vs. I/R values; ^e*P* < 0.01 vs. baseline. ^fIn this experiment, the reperfusion value was 0.7 ± 0.04 gray level. ^gIn this experiment, the baseline values of each group were 1.5 ± 0.5 (-15 min), 2.2 ± 0.5 (0 min), and 2.0 ± 0.5 (3 min). ^hIn this experiment, the baseline values of each group were 9.12 ± 0.34 (-15 min), 9.45 ± 0.4 (0 min), and 10.3 ± 0.65 (3 min) mm.

served in vivo with the styryl dye FM1-43, which is virtually nonfluorescent in aqueous media but fluoresces brightly upon binding cell membranes (14). FM1-43 has been used extensively to detect exocytosis in neuronal (15-17) and non-neuronal (18,19) cells. Thus, we determined FM1-43 fluorescence in conjunction with intravital microscopy quantification of P-selectin expression in the well-established model of pressure-induced activation of lung microvasculature, a condition which predisposes to pulmonary edema (20). Furthermore, because increased concentrations of cytosolic Ca²⁺ have been implicated in the mechanism of exocytosis of a number of agonists (21) including pressure elevation (22), intracellular Ca²⁺ concentrations ([Ca²⁺]_i) were measured. A moderate pressure elevation was applied to avoid liquid extravasation and vascular injury, thus allowing the precise measurements of the fluorescent signal in intact endothelial cells. In this model, ITF1697 was infused at a rate of 0.5 µg/min, which corresponds to about 0.4 µg/kg/min based on pharmacokinetic

considerations (unpublished data on file at Italfarmaco).

Pressure-Induced P-Selectin Release by Endothelial Cells

Figure 5A shows P-selectin immunofluorescence in single capillary of perfused rat lungs. At P_{LA} of 5 cmH₂O, P-selectin expression was sparse (left). At P_{LA} of 15 cmH₂O, capillary immunofluorescence markedly increased, as indicated by the development of yellow-green pseudocolor (middle panel). Furthermore, peak immunofluorescence was located at capillary branch points similarly to FM1-43 fluorescence, where the majority of exocytosis takes place (see below). In contrast, when the same capillary was infused with ITF1697 (right panel) there were no changes of pseudocolor upon increase of pressure. Quantification of this data shows that P_{LA} elevation increased P-selectin expression by 42 ± 18 gray levels above baseline, whereas administration of ITF1697 before pressure elevation blocked this response by 85% (*P* < 0.05, *n* = 3).

Pressure-Induced Capillary Leukocyte Accumulation

Past data (10,23) and those shown above indicate that vascular pressure elevation increases the level of P-selectin in lung capillaries, contributing to leukocyte accumulation at the site of its release. Leukocyte accumulation was quantified by rhodamine 6G fluorescence and shown as normalized gray levels in the graph in Figure 5B. Increase of P_{LA} augmented capillary fluorescence compared with fluorescence at baseline. By contrast, such an increase in fluorescence did not occur in ITF1697-treated capillaries. On average, pressure elevation increased leukocyte accumulation 1.5-fold above baseline. Conversely, ITF1697 infusion before P_{LA} elevation suppressed this response almost completely (*P* < 0.05, *n* = 3).

Pressure-Induced Endothelial Cell Exocytosis

Vascular pressure elevation increases exocytosis, as indicated by increased FM1-43 fluorescence in capillary endothelial cells (10). Figure 5C shows

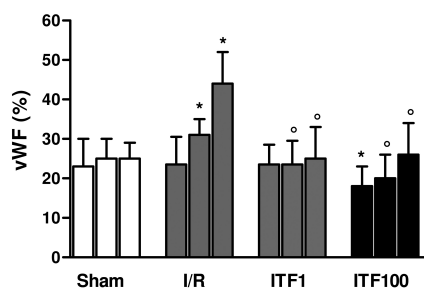


Figure 3. ITF1697 inhibits I/R-induced vWF release. vWF released into the plasma measured at baseline (white bars), at the end of ischemia (gray bars), and after reperfusion (black bars) in sham-operated animals and I/R and ITF1697 (1 and 100 $\mu\text{g}/\text{kg}/\text{min}$) groups. Values are means \pm SD, $n = 10$ animals per group. * $P < 0.001$ vs. baseline; $^{\circ}P < 0.05$ vs. the I/R group.

pseudocolor-coded capillary images. At $P_{\text{LA}} = 5 \text{ cmH}_2\text{O}$ (left upper panel), FM1-43 fluorescence (red) was sparse. In response to high P_{LA} (right upper panel), endothelial cells showed a marked increase of fluorescence representing increase of exocytosis. This pressure-induced fluorescence increase was predominantly located at capillary branch points. In contrast, the lower panel shows that P_{LA} elevation did not induce the increase of FM1-43 fluorescence in an ITF1697-treated capillary. The digital quantification showed that at $P_{\text{LA}} = 5 \text{ cmH}_2\text{O}$, fluorescence was negligible in both control and ITF1697-treated conditions. Increase of P_{LA} to $15 \text{ cmH}_2\text{O}$ increased FM1-43 fluorescence 12-fold in controls, but not in ITF1697-treated capillaries ($P < 0.05$, $n = 3$), indicating that ITF1697 infusion abolished pressure-induced increase of exocytosis.

Pressure-Induced (Ca^{2+})_i Oscillation in Endothelial Cells

$[\text{Ca}^{2+}]_i$ is a key factor in determining vascular exocytosis of P-selectin in response to a variety of stimuli (24). Therefore we quantified $[\text{Ca}^{2+}]_i$ in endothelial cells in perfused rat lung using fura-2 fluorescence assay. As shown in

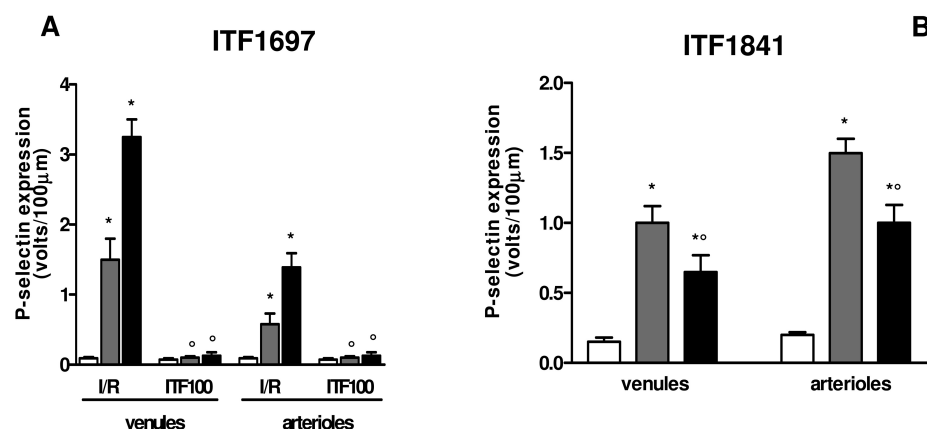


Figure 4. ITF1697 but not ITF1841 prevents I/R-induced P-selectin expression. (A) P-selectin expression in venules and arterioles measured at baseline (white bars) and after 15 min (gray bars) and 30 min (black bars) reperfusion in the I/R group in animals treated with ITF1697 at the dose of 100 $\mu\text{g}/\text{kg}/\text{min}$. (B) P-selectin expression in venules and arterioles of animals subjected to I/R and treated with ITF1841. P-selectin was measured at the end of reperfusion in control animals (gray bars) and in ITF1841-treated animals (black bars). Fluorescence is expressed in volts/100 μm of venules or arterioles. Values are means \pm SD, $n = 30$ for each entry. * $P < 0.001$ vs. baseline, $^{\circ}P < 0.05$ vs. the I/R group.

Figure 5D, high P_{LA} markedly increased $[\text{Ca}^{2+}]_i$ oscillation in vessels. In the presence of ITF1697, the pressure increase caused no change of fura-2 fluorescence compared with baseline, indicating that the peptide inhibited $[\text{Ca}^{2+}]_i$ oscillation. As shown in Figure 5D, ITF1697 greatly reduced the amplitude of $[\text{Ca}^{2+}]_i$ oscillation, indicating stabilization of $[\text{Ca}^{2+}]_i$ in treated vessels.

DISCUSSION

In this study, we show that ITF1697, a metabolically stabilized tetrapeptide of sequence Gly-(N α -Et)Lys-Pro-Arg, is highly efficacious in reducing microvascular inflammation and platelet aggregation in two models of microvascular injury, namely I/R in the hamster cheek pouch and high-pressure-induced endothelial activation in isolated rat lung preparations.

In the I/R model, treatment with ITF1697 inhibited leukocyte adhesion to venules (Figure 1D) and platelet adhesion to arterioles and venules (Figure 1C). These effects contributed significantly to preventing vasoconstriction in arterioles (Figure 1) and to maintaining

capillary perfusion during reperfusion (Figure 1A). ITF1697 inhibited I/R-induced microvascular permeability (Figure 1B) and maintained wall shear stress at basal levels (Table 1). The activity of the peptide appeared to be specific, as ITF1841, the des-Arg derivative and main ITF1697 metabolite, was only marginally efficacious on the vascular parameter changes induced by I/R.

Vascular protection by ITF1697 does not appear to require de novo synthesis of proteins, as indicated by time course experiments where maximal protection was achieved when the drug was administered during the early stages of I/R-induced endothelial activation. Rather, the mechanism of protection involves the inhibition of I/R-induced P-selectin expression (Figure 4A) and vWF release (Figure 3) from endothelial cells. The role of P-selectin and vWF in I/R is well documented. Reperfusion following ischemia is characterized by inflammatory responses in which P-selectin-dependent leukocyte recruitment occurs in the post-capillary venules (25-28). Platelets also adhere to the vessel wall by binding P-selectin and vWF expressed on the cell

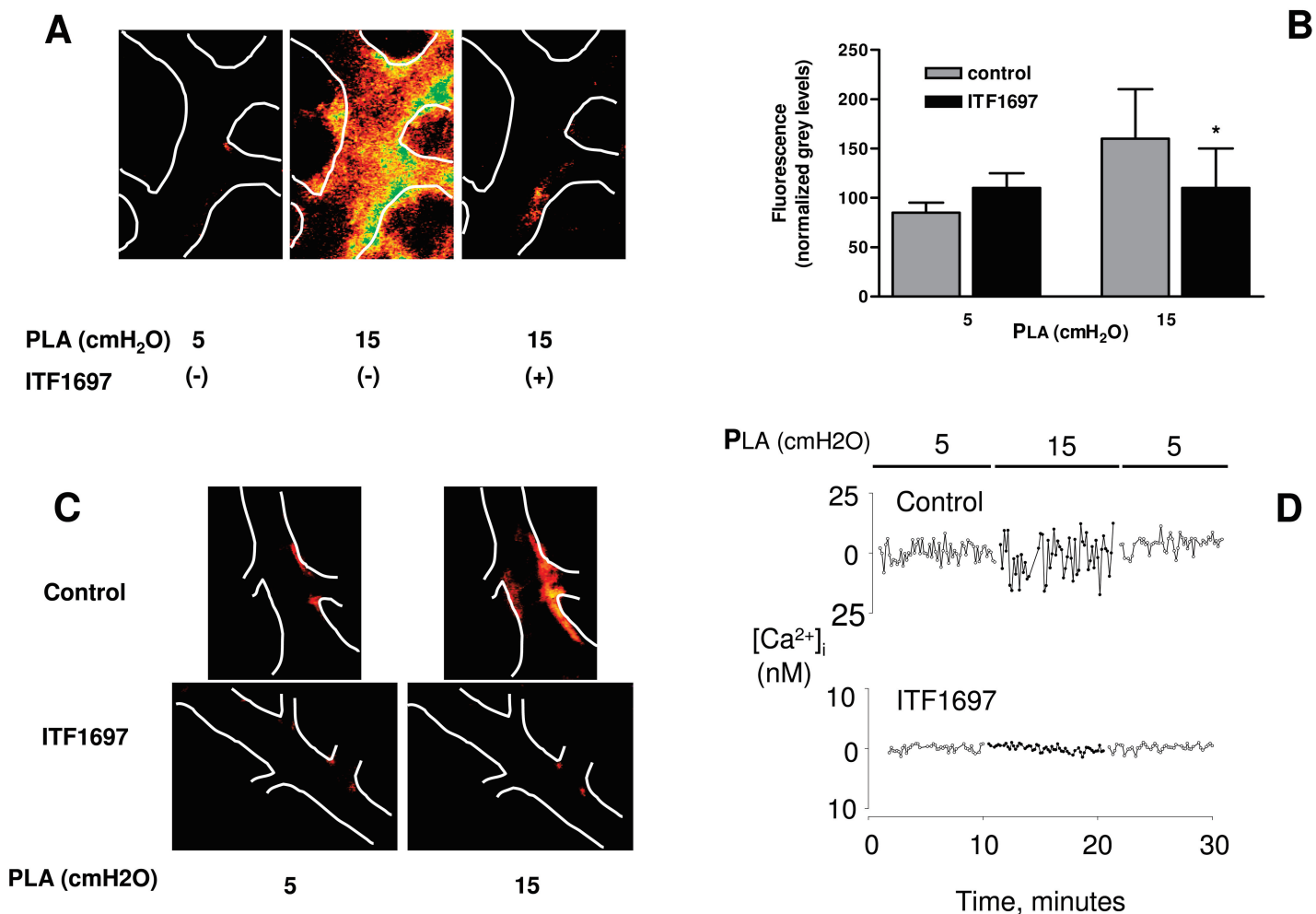


Figure 5. ITF1697 inhibits capillary endothelial cell activation of blood-perfused rat lungs. (A) Microscopic photograph of P-selectin-associated fluorescence in single capillaries. Images show marked increase of P-selectin-associated fluorescence upon increasing P_{LA} from 5 (left) to 15 (middle) cmH_2O . In a capillary given ITF1697 infusion (right panel), the pressure-induced P-selectin expression is prevented. (B) Leukocytes were stained by Rhodamine 6G infusion and their accumulation on capillary endothelial cells was quantified by fluorescence microscopy. The graph shows quantification of leukocyte accumulation as normalized gray levels. (C) Microscopic photograph of fluorescence dye exocytosed by lung capillaries. At $P_{LA} = 5$ cmH_2O (left upper panel), FM1-43 fluorescence (red pseudocolor) was sparse. Increase of P_{LA} to 15 cmH_2O (right upper panel) markedly increased the fluorescence, indicating increase of exocytosis. In contrast, ITF1697 perfusion (right lower panel) prevented capillary exocytosis. (D) Cytosolic Ca^{2+} concentration ($[Ca^{2+}]_i$) in capillary endothelial cells was quantified using fura-2 radiometric imaging technique. The graph shows the quantification of pressure-induced (Ca^{2+})_i oscillation amplitude as derived from fluorescence analysis. ITF1697 infusion inhibited the increase of (Ca^{2+})_i by 77% (* $P < 0.05$, $n = 3$).

surface of stimulated endothelium (29,30). Furthermore, vWF-mediated microvascular occlusion by platelet aggregates contributes to the failure of capillary perfusion following I/R injury (31-33). Consistent with these notions, inhibition of I/R-induced P-selectin expression and vWF release following treatment with the peptide was associated with the inhibition of endothelial

platelet and leukocyte adhesion (Figure 1C, D) and of capillary occlusion by platelet aggregates (Figure 2D). As expected, a specific antibody to P-selectin was also efficacious in reducing platelet and leukocyte adhesion to the vessel lumen (Figure 1C, D), although its protection on capillary perfusion was inferior to that of ITF1697 (Figure 1A). This is consistent with the additional effect

that ITF1697 has on the release of vWF that is not shared by the anti-P selectin antibody. Collectively, these observations suggest that the main target of the peptide is the exocytosis of WP bodies where vWF and P-selectin are stored.

We tested this hypothesis by additional studies in the model of pressure-induced endothelial activation in isolated lung preparations. We first demonstrated

that the mechanisms of protection in this model and in the I/R model are similar by showing that P-selectin expression and leukocyte adhesion to lung microcirculation are inhibited by treatments with the peptide (Figures 5A and B). Subsequent experiments showed that the peptide is able to inhibit the $[Ca^{2+}]_i$ increase-dependent fusion of WP bodies to the plasma membrane of endothelial cells (Figures 5C and D), confirming the hypothesis of inhibition of WP body exocytosis in the presence of ITF1697.

The WP body is the best characterized of the endothelial cell secretory granules and has long been recognized as intracellular storage not only for vWF and P-selectin (34), but also for interleukin-8, endothelin, and angiopoietin-2 (35), which contribute to the early responses of activated endothelium. The exocytosis of WP bodies is more prominent at venular bifurcations, concomitant with an increased cytosolic Ca^{2+} concentration (10,11). The same pattern was observed in our models, where the distribution of P-selectin appears to predominantly locate at venular bifurcations during reperfusion and exocytosis is seen at activated venular branch-points (Figure 5C). This confirms that the bifurcation is the main/first site of injury and adds support to our conclusion of ITF1697 as an inhibitor of $[Ca^{2+}]_i$ -dependent WP body exocytosis.

In conclusion, the combined evidence presented in this study suggests that ITF1697 is able to maintain normal arteriolar responses and capillary perfusion during post-ischemic reperfusion by inhibiting the calcium-dependent exocytosis of WP bodies. The regulated secretion of WP bodies provides a means by which endothelial cells can very rapidly alter the microenvironment of individual vascular beds and modulate the interrelated processes of coagulation, fibrinolysis, and inflammation. Therefore, the ability of ITF1697 to inhibit the early functions of activated endothelial cells represents a novel and promising pharmacological tool in pathologies involving abnormal microcirculation activation, including

prevention of re-occlusion after angioplasty and acute rejection in allo- and xenotransplantation.

Phase II clinical trials in patients undergoing percutaneous transluminal coronary angioplasty with or without coronary stenting have been carried out (36,37). These studies demonstrated that the peptide is well tolerated. Furthermore, although the population size of each treatment group was too small for a definite conclusion, a trend toward reperfusion improvement was seen in either a subgroup population or in a pilot study where efficacy of the peptide was assessed by radionuclide imaging (36,37).

REFERENCES

- Siemion IZ, Kluczyk A. (1999) Tuftsin: on the 30-year anniversary of Victor Najjar's discovery. *Peptides* 20:645-74.
- Catania A, Lipton JM. (1993) alpha-Melanocyte stimulating hormone in the modulation of host reactions. *Endocr. Rev.* 14:564-76.
- Ferreira SH, Lorenzetti BB, Bristow AF, Poole S. (1988) Interleukin-1 beta as a potent hyperalgesic agent antagonized by a tripeptide analogue. *Nature* 334:698-700.
- Robey F, et al. (1987) Proteolysis of human C-reactive protein produces peptides with potent immunomodulating activity. *J. Biol. Chem.* 262:7053-7.
- Fiedel BA. (1988) Influence of tuftsin-like synthetic peptides derived from C-reactive protein (CRP) on platelet behavior. *Immunology* 64:487-93.
- Caretto P, et al. (1995) Oligopeptides derived from C-reactive protein fragments. International Patent publ. no. WO 95/10531.
- Bertuglia S, Colantuoni A. (2000) Protective effects of leukopenia and tissue plasminogen activator in microvascular ischemia-reperfusion injury. *Am. J. Physiol. Heart Circ. Physiol.* 278:H755-61.
- Bertuglia S, Giusti A, Fedele S, Picano E. (2001) Glucose-insulin-potassium treatment in combination with dipyridamole inhibits ischaemia-reperfusion-induced damage. *Diabetologia* 44:2165-70.
- Bhattacharya J, Gropper MA, Shepard JM. (1989) Lung expansion and the perialveolar interstitial pressure gradient. *J. Appl. Physiol.* 66:2600-5.
- Kuebler WM, Ying X, Singh B, Issekutz AC, Bhattacharya J. (1999) Pressure is proinflammatory in lung venular capillaries. *J. Clin. Invest.* 104:495.
- Bertuglia S, Giusti A. (2002) Blockade of P-selectin does not affect reperfusion injury in hamsters subjected to glutathione inhibition. *Microvasc. Res.* 64:56-64.
- Lipowsky HH, Zweifach BW. (1978) Application of the "two-slit" photometric technique to the measurement of microvascular volumetric flow rates. *Microvasc. Res.* 15:93-101.
- Weyrich AS, Buerke M, Albertine KH, Lefer AM. (1995) Time course of coronary vascular endothelial adhesion molecule expression during reperfusion of the ischemic feline myocardium. *J. Leukoc. Biol.* 57:45-55.
- Betz WJ, Mao F, Bewick GS. (1992) Activity-dependent fluorescent staining and destaining of living vertebrate motor nerve terminals. *J. Neurosci.* 12:363-75.
- Betz WJ, Bewick GS. (1992) Optical analysis of synaptic vesicle recycling at the frog neuromuscular junction. *Science* 255:200-3.
- Hay M, Hasser EM. (1998) Measurement of synaptic vesicle exocytosis in aortic baroreceptor neurons. *Am. J. Physiol. Heart Circ. Physiol.* 275:H710-6.
- Kraszewski K, Daniell L, Mundigl O, De Camilli P. (1996) Mobility of synaptic vesicles in nerve endings monitored by recovery from photobleaching of synaptic vesicle-associated fluorescence. *J. Neurosci.* 16:5905-13.
- Giovannucci DR, Yule DI, Stuenkel EL. (1998) Optical measurement of stimulus-evoked membrane dynamics in single pancreatic acinar cells. *Am. J. Physiol. Cell Physiol.* 275:C732-9.
- Smith CB, Betz WJ. (1996) Simultaneous independent measurement of endocytosis and exocytosis. *Nature* 380:531-4.
- Bhattacharya J. (1998) Physiological basis of pulmonary edema. In: Matthay MA, Ingbar DH (eds.) *Pulmonary Edema*. Marcel Dekker Inc., New York, p. 1-36.
- Datta YH, Ewenstein BM. (2001) Regulated secretion in endothelial cells: biology and clinical implications. *Thromb. Haemost.* 86:1148-55.
- Ichimura H, Parthasarathi K, Quadri S, Issekutz AC, Bhattacharya J. (2003) Mechano-oxidative coupling by mitochondria induces proinflammatory responses in lung venular capillaries. *J. Clin. Invest.* 111:691.
- Ichimura H, Parthasarathi K, Issekutz AC, Bhattacharya J. (2005) Pressure-induced leukocyte margination in lung postcapillary venules. *Am. J. Physiol. Lung Cell Mol. Physiol.* 289:L407-12.
- Birch KA, Ewenstein BM, Golan DE, Pober JS. (1994) Prolonged peak elevations in cytoplasmic free calcium ions, derived from intracellular stores, correlate with the extent of thrombin-stimulated exocytosis in single human umbilical vein endothelial cells. *J. Cell Physiol.* 160:545-54.
- Eppihimer M, Granger D. (1997) Ischemia/reperfusion-induced leukocyte-endothelial interactions in postcapillary venules. *Shock* 8:16-25.
- Jerome SN, Akimitsu T, Korthisuis RJ. (1994) Leukocyte adhesion, edema, and development of postischemic capillary no-reflow. *Am. J. Physiol. Heart Circ. Physiol.* 267:H1329-36.
- Lefer A, Weyrich A, Buerke M. (1994) Role of selectins, a new family of adhesion molecules, in ischaemia-reperfusion injury. *Cardiovasc. Res.* 28:289-94.

28. Mayadas TN, Johnson RC, Rayburn H, Hynes RO, Wagner DD. (1993) Leukocyte rolling and extravasation are severely compromised in P-selectin-deficient mice. *Cell* 74:541-54.
29. Cambien B, Wagner DD. (2004) A new role in hemostasis for the adhesion receptor P-selectin. *Trends Mol. Med.* 10:179-86.
30. Andre P, et al. (2000) Platelets adhere to and translocate on von Willebrand factor presented by endothelium in stimulated veins. *Blood* 96:3322-8.
31. Gawaz M, Langer H, May AE. (2005) Platelets in inflammation and atherogenesis. *J. Clin. Invest.* 115:3378-84.
32. Xu Y, et al. (2006) Activated platelets contribute importantly to myocardial reperfusion injury. *Am. J. Physiol. Heart Circ. Physiol.* 290:H692-9.
33. Massberg S, et al. (1998) Platelet-endothelial cell interactions during ischemia/reperfusion: the role of P-selectin. *Blood* 92:507-15.
34. Michaux G, Cutler DF. (2004) How to roll an endothelial cigar: the biogenesis of Weibel-Palade bodies. *Traffic* 5:69-78.
35. Rondaj MG, Bierings R, Kragt A, van Mourik JA, Voorberg J. (2006) Dynamics and plasticity of Weibel-Palade bodies in endothelial cells. *Arterioscler. Thromb. Vasc. Biol.* 26:1002-7.
36. Syeda B, et al. (2004) Assessment of the safety and efficacy of the novel tetrapeptide ITF-1697 on infarct size after primary PTCA in acute myocardial infarction: a randomised, placebo-controlled pilot trial. *Drugs R. D.* 5:141-51.
37. Dirksen MT, et al. (2004) The effect of ITF-1697 on reperfusion in patients undergoing primary angioplasty: safety and efficacy of a novel tetrapeptide, ITF-1697. *Eur. Heart J.* 25:392-400.